Journal of Guidance, Control, and Dynamics, Vol. 41, No. 4, 2018, pp. 1009–1014. doi: http://doi.org/10.2514/1.G003088

Relative Motion of Sun-pointing Smart Dust in Circular Heliocentric Orbits

Giovanni Mengali* Alessandro A. Quarta† and Eugenio Denti‡
Department of Civil and Industrial Engineering, University of Pisa, I-56122 Pisa, Italy

Nomenclature

$\mathbb{A}$	=	constant matrix $\in \mathbb{R}^{4\times 4}$
$\boldsymbol{a}$	=	SD propulsive acceleration, [mm/s^2]
a, b, c	=	auxiliary variable
$\mathbb{B}, \mathbb{C}$	=	constant vector $\in \mathbb{R}^{4\times 1}$
$\mathbb{D}$	=	time-dependent matrix $\in \mathbb{R}^{4\times 4}$
$\mathbb{E}, \mathbb{F}, \mathbb{K}$	=	time-dependent vector $\in \mathbb{R}^{4\times 1}$
H	=	Heaviside step function
r	=	Sun-spacecraft distance, [au]
T	=	orbital period, [days]
t	=	time, [days]
u, v	=	radial and transverse relative velocity, [km/s]
$\boldsymbol{x}$	=	state vector
β	=	lightness number
$\Delta\beta$	=	lightness number variation
ϵ	=	error
$\mu_\odot$	=	Sun's gravitational parameter, [au^3/day^2]
τ	=	switching parameter
ϕ	=	phasing angle, [deg]
ω	=	angular velocity, [rad/s]

Subscripts

0	=	initial
c	=	circular MS orbit
des	=	design
max	=	maximum
min	=	minimum
off	=	ECS off
on	=	ECS on

Superscripts

$-$	=	mean value
$\cdot$	=	time derivative
$\wedge$	=	unit vector

Introduction

A Smart Dust (SD) is an innovative and fascinating femto-spacecraft concept, with a characteristic side length of some centimeters or even some millimeters, whose external surface is coated with electrochromic material. A SD can be thought of as the evolution of the so-called spacecraft-on-a-chip [1, 2], that is, an integrated-circuit silicon spacecraft with a characteristic dimension of a few millimeters and a mass on the order of a few grams. A SD is characterized by high values of area-to-mass ratio, and so the solar radiation pressure acting on it produces a significant propulsive acceleration, sufficient for modifying its space trajectory [3–5]. As the optical properties of the electrochromic material change with the application of a suitable voltage, the SD propulsive acceleration may be modulated within some limits.

There exist many different and potentially interesting applications for SDs, including the possibility of obtaining distributed sensor networks for planetary observation [6, 7], or that of generating a support and a communication system for conventional spacecraft operating in the interplanetary space [8, 9]. A feature of great interest is the reduced size of these objects, which could be effectively exploited to stow a number of SDs within a single Mother Ship (MS) of small dimensions, such as a CubeSat [10, 11], thus substantially reducing the launch costs. The SDs could be released from the MS and then adjusted to operate near it for a desired time-interval, to create a monitoring system with diagnostic purposes.

In a recent paper, the authors [12] have studied the heliocentric dynamics of a Sun-pointing SD, that is, a SD that provides (through a suitable design of the external shape) an outward propulsive acceleration directed along the Sun-SD line. The propelled heliocentric trajectory of such a femto-spacecraft has been described, using a linear systems approach, as a function of the optical properties of the electrochromic material. The aim of this Note is to extend the results of Ref. [12] to the study of the linearized relative motion of a Sun-pointing SD and a MS when the latter describes a circular heliocentric orbit. More precisely, assuming the Sun-SD distance to be close to the MS orbital radius, the linearized relative dynamics between SD and

*Professor, g.mengali@ing.unipi.it. Senior Member AIAA.
†Associate Professor, a.quarta@ing.unipi.it. Associate Fellow AIAA (**corresponding author**).
‡Associate Professor, e.denti@ing.unipi.it.

MS is described with an approach similar to that used by McInnes [13] in the analysis of the azimuthal repositioning problem for a solar sail-based spacecraft. The contribution in the study to follow is therefore different from that discussed in Ref. [12], whose aim, instead, is to find the SD heliocentric trajectory as a function of a given control law. The results about the SD-MS relative dynamics are obtained in an analytical form and are applied to a phasing mission case [14,15], a scenario in which the SD varies its angular position (along the circular reference orbit) with respect to that of the MS.

Mathematical Model

Consider a MS that covers a heliocentric circular (Keplerian) orbit of radius r_c, with a constant angular velocity $\omega = \sqrt{\mu_\odot / r_c^3}$, where $\mu_\odot$ is the Sun's gravitational parameter, see Fig. 1. At a certain time the MS releases a SD, whose distance from the Sun is assumed to remain close to r_c. The problem is to study the MS-SD relative trajectory and to obtain an analytical model suitable for quantifying the angular displacement between the two spacecraft as a function of time.

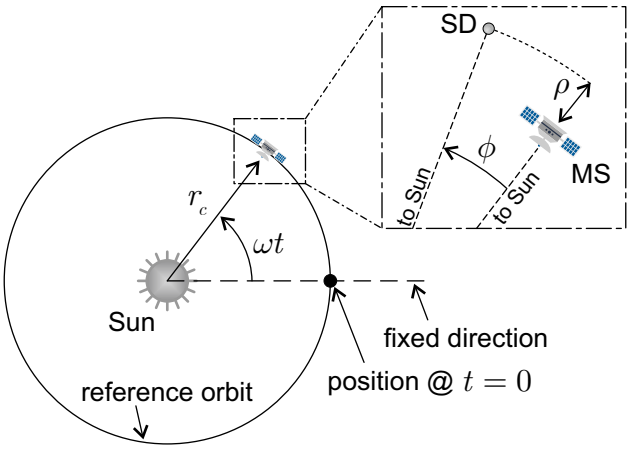

Figure 1 Reference frame and state variables.

The propulsive acceleration $\boldsymbol{a}$ of a Sun-pointing SD with an active Electrochromic-based Control System (ECS) [12], at a distance r from the Sun, can be modelled as a radial modulated (outward) acceleration in the form

$$\boldsymbol{a} = \beta \, \frac{\mu_\odot}{r^2} \, \hat{\boldsymbol{r}} \tag{1}$$

where $\hat{\boldsymbol{r}}$ is the Sun-SD unit vector, and β is the SD lightness number, defined as the ratio between the value of $\|\boldsymbol{a}\|$ to the modulus of the local Sun's gravitational acceleration. When operated by a suitable voltage, the reflectivity coefficient of the electrochromic material coated on the SD external surface is assumed to take two admissible values, which implies $\beta = \beta_{\min} > 0$ (power-off state) or $\beta = \beta_{\max} \geq \beta_{\min}$ (power-on state). Accordingly, the SD propulsive acceleration can be written as

$$\boldsymbol{a} = (\beta_{\min} + \tau \, \Delta\beta) \, \frac{\mu_\odot}{r^2} \, \hat{\boldsymbol{r}} \tag{2}$$

where $\Delta\beta \triangleq \beta_{\max} - \beta_{\min} \geq 0$ is the variation in the SD lightness number due to the ECS, and $\tau = \tau(t) \in \{0, 1\}$ is a (time-dependent) switching parameter that models the on/off behaviour of the ECS. Assuming that the ECS is switched on (or off) at time t_{on_i} (or t_{off_i}), with $i \in \mathbb{N}$ and $t_{\mathrm{off}_i} > t_{\mathrm{on}_i}$, the time variation of the switching parameter can be written in a compact form as

$$\tau(t) = \sum_{i=1}^{n} H(t - t_{\mathrm{on}_i}) - \sum_{i=1}^{n} H(t - t_{\mathrm{off}_i}) \tag{3}$$

where $n \geq 1$ is the number of working cycles of the electrochromic material (that is, the number of on-off switchings of the ECS), whereas $H(y)$ is the Heaviside step function, that is, $H(y) = 0$ if $y < 0$, and $H(y) = 1$ if $y \geq 0$. Equation (3) describes the SD discontinuous control law, according to which the local propulsive acceleration modulus $\|\boldsymbol{a}\|$ can take two possible values only, corresponding to either $\beta = \beta_{\min}$ or $\beta = \beta_{\max}$.

The lightness numbers $\beta_{\min}$ and $\beta_{\max}$ (and, so the value of $\Delta\beta$) depend on the optical characteristics of the electrochromic material and on the SD area-to-mass ratio. For a given SD mass and shape, the minimum (or maximum) value of β is obtained when the electrochromic film absorbs (or specularly reflects) all of the incident electromagnetic radiation. Typical values of the SD lightness number for a low-performance (SD_1), medium-performance (SD_2), and high-performance (SD_3) configuration are summarized in Tab. 1, which takes into account the real optical characteristics of the electrochromic material [5].

	SD_1	SD_2	SD_3
$\beta_{\min}$	0.0134	0.0251	0.0420
$\beta_{\max}$	0.0241	0.0451	0.0756
$\Delta\beta$	0.0107	0.0201	0.0336

Table 1 Lightness number of a low (SD_1), medium (SD_2), and high (SD_3) performance smart dust. Data adapted from Ref. [5].

According to McInnes [13], as long as the SD heliocentric trajectory is sufficiently close to the circular orbit tracked by the MS, the relative SD-MS dynamics can be described by the following linearized differential equations

$$\dot{\rho} = u \tag{4}$$

$$\dot{\phi} = \frac{v}{r_c} \tag{5}$$

$$\dot{u} = 2\,\omega\,v + 3\,\omega^2\,\rho + (\beta_{\min} + \tau\,\Delta\beta)\;\frac{\mu_\odot}{r_c^2} \tag{6}$$

$$\dot{v} = -2\,\omega\,u \tag{7}$$

where ρ is the difference between the Sun-SD distance and the Sun-MS distance (with $|\rho| \ll r_c$), ϕ is the SD-MS relative angular coordinate, and u (or v) is the radial (or transverse) component of the SD-MS relative velocity, see Fig. 1. The only control parameter is τ, whose time-variation is described by Eq. (3). Note that Eqs. (4)–(7) are consistent with the mathematical model discussed in Ref. [15]. In the limiting case when an ECS failure occurs before the SD deployment, $\Delta\beta \equiv 0$ in Eq. (6) and the SD experiences an outward, radial, propulsive acceleration of modulus $\beta_{\min}\,\mu_\odot/r^2$ for all $t \geq 0$, see Eq. (1).

The linear time-invariant system of Eqs. (4)-(7) can be written in a compact form as

$$\dot{\boldsymbol{x}} = \mathbb{A}\,\boldsymbol{x} + \tau\,\mathbb{B} + \mathbb{C} \tag{8}$$

where $\boldsymbol{x} \triangleq [\rho,\, \phi,\, u,\, v]^{\mathrm{T}}$ is the state vector, while the constant matrices $\mathbb{A} \in \mathbb{R}^{4\times4}$ and $\{\mathbb{B}, \mathbb{C}\} \in \mathbb{R}^{4\times1}$ are defined as

$$\mathbb{A} \triangleq \begin{bmatrix} 0 & 0 & 1 & 0 \\ 0 & 0 & 0 & 1/r_c \\ 3\,\omega^2 & 0 & 0 & 2\,\omega \\ 0 & 0 & -2\,\omega & 0 \end{bmatrix} \quad , \quad \mathbb{B} \triangleq \begin{bmatrix} 0 \\ 0 \\ \Delta\beta\,r_c\,\omega^2 \\ 0 \end{bmatrix} \quad , \quad \mathbb{C} \triangleq \begin{bmatrix} 0 \\ 0 \\ \beta_{\min}\,r_c\,\omega^2 \\ 0 \end{bmatrix}$$

The differential equation (8) can be solved with standard methods, and the result is

$$\boldsymbol{x}(t) = \mathbb{D}(t)\,\boldsymbol{x}_0 + \mathbb{E}(t) + \Delta\beta \sum_{i=1}^{n} \{H(t - t_{\mathrm{on}_i})\,\mathbb{F}(t, t_{\mathrm{on}_i}) - H(t - t_{\mathrm{off}_i})\;\mathbb{F}(t, t_{\mathrm{off}_i})\} \tag{9}$$

where

$$\mathbb{D}(t) \triangleq \begin{bmatrix} [4 - 3\cos(\omega t)] & 0 & \dfrac{\sin(\omega t)}{\omega} & \dfrac{2\,[1 - \cos(\omega t)]}{\omega} \\ \dfrac{6\,[\sin(\omega t) - \omega t]}{r_c} & 1 & \dfrac{2\,[\cos(\omega t) - 1]}{\omega\,r_c} & \dfrac{4\,\sin(\omega t) - 3\,\omega\,t}{\omega\,r_c} \\ 3\,\omega\,\sin(\omega t) & 0 & \cos(\omega t) & 2\,\sin(\omega t) \\ 6\,\omega\,[\cos(\omega t) - 1] & 0 & -2\,\sin(\omega t) & 4\,\cos(\omega t) - 3 \end{bmatrix} \tag{10}$$

$$\mathbb{E}(t) \triangleq \beta_{\min} \begin{bmatrix} r_c\,[1 - \cos(\omega t)] \\ 2\,[\sin(\omega t) - \omega t] \\ \omega\,r_c\,\sin(\omega t) \\ 2\,\omega\,r_c\,[\cos(\omega t) - 1] \end{bmatrix} \tag{11}$$

$$\mathbb{F}(t, y) \triangleq \begin{bmatrix} r_c\,[1 - \cos(\omega t - \omega y)] \\ 2\,[\sin(\omega t - \omega y) - \omega t + \omega y] \\ \omega\,r_c\,\sin(\omega t - \omega y) \\ 2\,\omega\,r_c\,[\cos(\omega t - \omega y) - 1] \end{bmatrix} \tag{12}$$

and $\boldsymbol{x}_0$ is the state vector at the initial time $t_0 \triangleq 0$. The MS-SD (approximate) relative trajectory may therefore be studied with the aid of Eq. (9) as a function of the initial conditions $\boldsymbol{x}_0$ and the control time-history $\tau(t)$ given by Eq. (3).

Maximum distance of the SD from the reference orbit

The linearized equations of motions (4)-(7) have been obtained under the assumption that the Sun-SD distance is close to the radius of the circular orbit of the MS [13], that is, $|\rho|\,/r_c \ll 1$, see Fig. 1. An estimate of the maximum value of $|\rho|\,/r_c$ can be obtained by observing that, from Eq. (9), the time variation of ρ is given by

$$\rho(t) = a + b\,\cos(\omega t) + c\,\sin(\omega t) \tag{13}$$

where

$$a \triangleq 4\,\rho_0 + \beta_{\min}\,r_c + \frac{2\,v_0}{\omega} + \Delta\beta\,r_c \sum_{i=1}^{n}\{H(t-t_{\mathrm{on}_i}) - H(t-t_{\mathrm{off}_i})\} \tag{14}$$

$$b \triangleq -\frac{2\,v_0}{\omega} - 3\,\rho_0 - \beta_{\min}\,r_c + \Delta\beta\,r_c \sum_{i=1}^{n}\{H(t-t_{\mathrm{off}_i})\,\cos(\omega\,t_{\mathrm{off}_i}) - H(t-t_{\mathrm{on}_i})\,\cos(\omega\,t_{\mathrm{on}_i})\} \tag{15}$$

$$c \triangleq \frac{u_0}{\omega} + \Delta\beta\,r_c \sum_{i=1}^{n}\{H(t-t_{\mathrm{off}_i})\,\sin(\omega\,t_{\mathrm{off}_i}) - H(t-t_{\mathrm{on}_i})\,\sin(\omega\,t_{\mathrm{on}_i})\} \tag{16}$$

from which it may be verified that

$$|\rho|\,/r_c \le 7\,|\rho_0|\,/r_c + 2\,\beta_{\min} + \frac{4\,|v_0| + |u_0|}{\omega\,r_c} + \Delta\beta\,(4\,n+1) \tag{17}$$

This last inequality provides a conservative estimate of the maximum radial distance $|\rho|_{\max}$ of the SD from the circular orbit of radius r_c, as a function of the initial conditions and the control inputs.

Special cases

A particularly simple mission example occurs when the SD deployment takes place at time t_0 with zero relative velocity with respect to the MS. This case corresponds to zero initial conditions, or $\boldsymbol{x}_0 = 0$. Assuming an ECS failure before the SD deployment (i.e., $\Delta\beta = 0$), Eq. (9) reduces to

$$\boldsymbol{x}(t) = \mathbb{E}(t) \tag{18}$$

where $\mathbb{E}$ is given by Eq. (11). In this case the time history of the relative radial distance is

$$\rho(t) = \beta_{\min}\,r_c\,[1-\cos(\omega\,t)] \quad \text{if} \quad \{\Delta\beta,\,\boldsymbol{x}_0\} = 0 \tag{19}$$

which is always nonnegative and takes a maximum value

$$\rho_{\max} = 2\,\beta_{\min}\,r_c \tag{20}$$

which agrees with Eq. (17) when $\{\rho_0,\,u_0,\,v_0,\,\Delta\beta\} = 0$. From Eqs. (11) and (18), the time history of the angular coordinate is

$$\phi(t) = 2\,\beta_{\min}\,[\sin(\omega\,t) - \omega\,t] \quad \text{if} \quad \{\Delta\beta,\,\boldsymbol{x}_0\} = 0 \tag{21}$$

which is negative for all $t > 0$, due to the secular term $2\,\beta_{\min}\,\omega\,t$. Let $T_c \triangleq 2\,\pi/\omega$ be the orbital period of the MS. It can be verified, with the aid of Eqs. (11)-(18), that $\rho(T_c) = 0$ and $u(T_c) = v(T_c) = 0$. In other terms, the SD comes back to the reference circular orbit (with zero relative velocity) after one orbital period, thus performing an in-orbit repositioning with a drift behind maneuver of an angle

$$\Delta\phi = \phi(T_c) = -4\,\pi\,\beta_{\min} \tag{22}$$

whose value, according to Eqs. (19)-(21), can be related to the maximum value of the ratio ρ/r_c as

$$\Delta\phi = -2\,\pi\,\frac{\rho_{\max}}{r_c} \tag{23}$$

Assume, for example, a circular reference orbit of radius $r_c = 1\,\mathrm{au}$ and consider the low-performance SD_1, whose main characteristics are reported in Tab. 1. When $\{\Delta\beta,\,\boldsymbol{x}_0\} = 0$, the time variations of the state variables are drawn in Fig. 2(a), whereas Fig. 2(b) illustrates the SD relative trajectory in a reference frame rotating around the Sun with an angular velocity equal to ω. In this case $T_c = 1\,\mathrm{year}$, and the SD angular coordinate varies of about $\Delta\phi \simeq -0.1684\,\mathrm{rad} \simeq -10\,\mathrm{deg}$ within one year, according to Eqs. (20) and (23). The corresponding maximum value of ρ is slightly less than 3% of r_c, see Eq. (20) and Fig. 2(a).

Equations (18)-(23) are also valid in the conceptually similar situation when the ECS is operating for all time, which amounts to formally substituting $\beta_{\min}$ with $\beta_{\max}$ in Eqs. (18)–(21). In the latter case the increased outward propulsive acceleration induces, as expected, an increase of both $\rho_{\max}$ and $|\Delta\phi|$ in a period T_c, see Eqs. (20) and (22). For example, using again the SD_1 case with $\beta = \beta_{\max} = 0.0241$, see Tab. 1, the phasing angle in a time interval $T_c = 1\,\mathrm{year}$ is $\Delta\phi = -4\,\pi\,\beta_{\max} \simeq -0.3028\,\mathrm{rad} \simeq -17\,\mathrm{deg}$ with $\rho_{\max}/r_c \simeq 4.8\%$.

Final relative trajectory

The analytical solution of Eq. (9) can be used to find the relative MS-SD trajectory when the ECS is finally switched off, that is, on completion of the n working cycles in Eq. (3). To this end, note that, when $t > t_{\mathrm{off}_n}$, $H(t-t_{\mathrm{on}_i}) \equiv H(t-t_{\mathrm{off}_i}) = 1$ with $i = 1, 2, \ldots, n$. The solution for $\boldsymbol{x}(t)$ is therefore formally similar to that written in Eq. (9), with the only exception of the last term in the right-hand side, which is now replaced by

$$\Delta\beta \sum_{i=1}^{n}\{\mathbb{K}(t,t_{\mathrm{on}_i}) - \mathbb{K}(t,t_{\mathrm{off}_i})\} \quad \text{with} \quad \mathbb{K}(t,y) \triangleq \begin{bmatrix} -r_c\,\cos(\omega t - \omega y) \\ 2\,[\sin(\omega t - \omega y) + \omega y] \\ \omega\,r_c\,\sin(\omega t - \omega y) \\ 2\,\omega\,r_c\,\cos(\omega t - \omega y) \end{bmatrix} \tag{24}$$

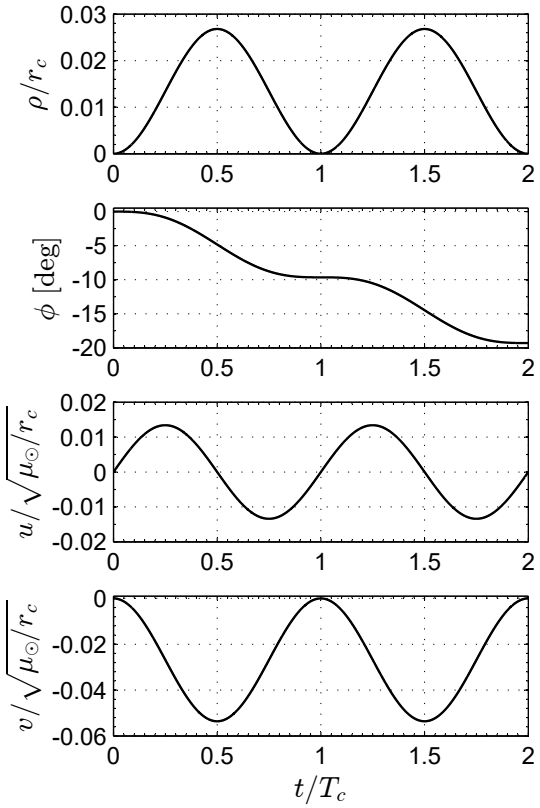

a) State variables.

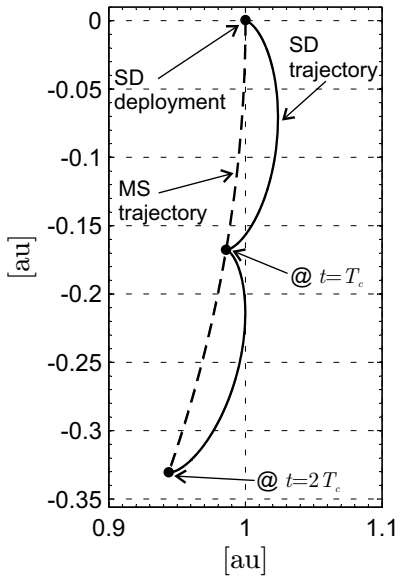

b) Relative trajectory.

Figure 2 Analytical results when $r_c = 1\,\mathrm{au}$ and $\beta_{\min} = 0.0134$ if $\{\Delta\beta,\, \boldsymbol{x}_0\} = 0$.

Control law design

Assuming a SD deployment with zero initial conditions ($\boldsymbol{x}_0 = 0$) and a constant lightness number $\beta \in \{\beta_{\min}, \beta_{\max}\}$, the relative SD-MS dynamics is described by Eq. (18). The SD goes back periodically to the circular reference orbit with zero relative velocity at any time interval $\Delta t = T_c$, thus performing a drift behind maneuver at a (constant) mean rate

$$\overline{\dot{\phi}} = \frac{\phi(\Delta t)}{\Delta t} \equiv \frac{\Delta\phi}{\Delta t} = -\frac{4\,\pi\,\beta}{T_c} \tag{25}$$

Therefore, there are only two admissible values of $\overline{\dot{\phi}}$, which correspond to the two possible values of the lightness number ($\beta = \beta_{\min}$ or $\beta = \beta_{\max}$). For example, using the data of Tab. 1, the mean rate is $\overline{\dot{\phi}} \simeq -\{10,\, 17\}$ deg/year for a SD_1, $\overline{\dot{\phi}} \simeq -\{18,\, 32\}$ deg/year for a SD_2 and $\overline{\dot{\phi}} \simeq -\{30,\, 54\}$ deg/year for a SD_3.

The situation is different when τ may be either turned on or off according to a suitable control law $\tau = \tau(t)$. For illustrative purposes, assume the control system to perform a single working cycle, that is, $n = 1$ in Eq. (3). In this simple case the time histories of the four state variables after the ECS is switched off (that is, when $t \geq t_{\mathrm{off}}$), are

$$\frac{\rho(t)}{r_c} = \beta_{\min}\,[1 - \cos(\omega\,t)] + \Delta\beta\,[\cos(\omega\,t - \omega\,t_{\mathrm{off}}) - \cos(\omega\,t - \omega\,t_{\mathrm{on}})] \tag{26}$$

$$\frac{u(t)}{\omega\,r_c} = \beta_{\min}\,\sin(\omega\,t) + \Delta\beta\,[\sin(\omega\,t - \omega\,t_{\mathrm{on}}) - \sin(\omega\,t - \omega\,t_{\mathrm{off}})] \tag{27}$$

$$\phi(t) = \frac{2\,u(t)}{\omega\,r_c} + 2\,\Delta\beta\,\omega\,(t_{\mathrm{on}} - t_{\mathrm{off}}) - 2\,\beta_{\min}\,\omega\,t \tag{28}$$

$$\frac{v(t)}{\omega\,r_c} = -2\,\frac{\rho(t)}{r_c} \tag{29}$$

The problem is to find the time instants t_{on} (when $\tau = 1$), t_{off} (when $\tau = 0$), and the time interval Δt necessary to complete the in-orbit repositioning maneuver, with final conditions $\rho(\Delta t) = 0$, $u(\Delta t) = v(\Delta t) = 0$, and $\phi(\Delta t)/\Delta t = \overline{\dot{\phi}}_{\mathrm{des}}$, where $\overline{\dot{\phi}}_{\mathrm{des}}$ is the desired mean rate-of-change of the (relative) azimuthal angle. Taking into account Eq. (28), when $u(\Delta t) = 0$ and $\phi(\Delta t)/\Delta t = \overline{\dot{\phi}}_{\mathrm{des}}$, it can be verified that the time fraction within which the ECS is switched on is a linear function of the desired mean rate-of-change of the azimuthal angle, viz.

$$\frac{t_{\mathrm{off}} - t_{\mathrm{on}}}{\Delta t} = -\frac{\overline{\dot{\phi}}_{\mathrm{des}}}{2\,\Delta\beta\,\omega} - \frac{\beta_{\min}}{\Delta\beta} \tag{30}$$

Bearing in mind Eqs. (26)-(29), the final conditions $\rho(\Delta t) = 0$ and $u(\Delta t) = v(\Delta t) = 0$ are obtained when (see also Fig. 3)

$$t_{\mathrm{on}} = \frac{\Delta t}{2} - \tilde{t} \qquad , \qquad t_{\mathrm{off}} = \frac{\Delta t}{2} + \tilde{t} \tag{31}$$

where $\tilde{t} \in [0, \Delta t/2]$ is defined as a function of Δt as

$$\tilde{t} = -\frac{1}{\omega}\,\arcsin\left(\frac{\beta_{\min}}{\Delta\beta}\,\sin\frac{\omega\,\Delta t}{2}\right) \tag{32}$$

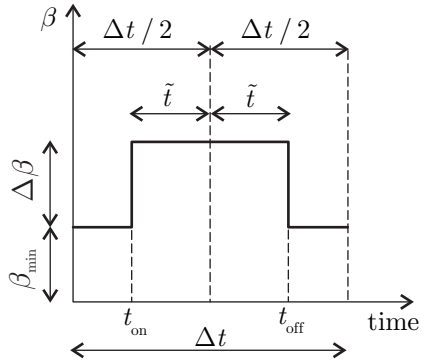

Figure 3 Lightness number time-history when $n = 1$.

The time interval Δt corresponding to the in-orbit repositioning problem is the solution of a nonlinear equation obtained by substituting Eqs. (31)-(32) into Eq. (30), viz.

$$\sin\left(\frac{\overline{\dot{\phi}}_{\mathrm{des}} + 2\,\omega\,\beta_{\min}}{4\,\Delta\beta}\,\Delta t\right) = \frac{\beta_{\min}}{\Delta\beta}\,\sin\left(\frac{\omega\,\Delta t}{2}\right) \tag{33}$$

which can be solved numerically, as a function of $\dot{\phi}_{\rm des}$, with standard methods. Note that, since $\omega = 2\,\pi/T_c$ and $\tilde{t} \geq 0$, Eq. (32) states that $\Delta t \geq T_c$.

Two special cases are worth noting. The first one is when $t_{\rm on} = \Delta t/2$, that is $\tilde{t} = 0$ and $t_{\rm off} = \Delta t/2$, see Eq. (31). From Eq. (32) it is found that $\Delta t = T_c$. In other terms, $t_{\rm on}/T_c = t_{\rm off}/T_c = 1/2$ and the ECS is always off, see also Fig. 3. From Eq. (28), the azimuthal angle decreases at a constant mean rate $\overline{\dot{\phi}} = -2\,\omega\,\beta_{\rm min} \equiv -4\,\pi\,\beta_{\rm min}/T_c$. The second special case is when $t_{\rm on} = 0$, that is $\tilde{t} = \Delta t/2$ and $t_{\rm off} = \Delta t$. Similar to the previous case, Eq. (32) states that $\Delta t = T_c$, which implies $t_{\rm off}/T_c = 1$ and the ECS is always on. Using again Eq. (28), the azimuthal angle decreases at a constant mean rate $\overline{\dot{\phi}} = -2\,\omega\,\beta_{\rm max} \equiv -4\,\pi\,\beta_{\rm max}/T_c$.

Figure 4(a) summarizes the results for the $\rm SD_1$ case as a function of $\overline{\dot{\phi}}_{\rm des}$. As expected, the extreme values of $\overline{\dot{\phi}}_{\rm des}$ correspond to when the ECS is always either switched off ($\beta = \beta_{\rm min}$) or on ($\beta = \beta_{\rm max}$). In the former case $t_{\rm on} \equiv t_{\rm off}$ and $\left|\overline{\dot{\phi}}_{\rm des}\right| = 4\,\pi\,\beta_{\rm min}\,{\rm rad/year} \simeq 10\,{\rm deg/year}$. In the second case $t_{\rm on} = 0$ and $t_{\rm off} = T_c$ (that is, the ECS is always on) and $\left|\overline{\dot{\phi}}_{\rm des}\right| = 4\,\pi\,\beta_{\rm max}\,{\rm rad/year} \simeq 17\,{\rm deg/year}$. Figure 4(b) shows the phasing angle $\phi(\Delta t)$ and the maximum radial distance from the reference orbit as a function of $\overline{\dot{\phi}}_{\rm des}$. In particular, $|\phi(\Delta t)|$ and $|\rho|_{\rm max}$ are both increasing functions of $\overline{\dot{\phi}}_{\rm des}$ and the maximum distance, equal to $2\,\beta_{\rm max}\,r_c$, is obtained when $\beta = \beta_{\rm max}$ for all time.

The information summarized in Fig. 4 may be effectively used for the preliminary design of an in-orbit repositioning maneuver for the $\rm SD_1$ case when $n = 1$. For illustrative purposes, assuming $|\rho|_{\rm max}/r_c \leq 3\%$, the mean rate-of-change of the azimuthal angle is $\left|\overline{\dot{\phi}}_{\rm des}\right| \leq 12\,{\rm deg/year}$. For example, taking $\overline{\dot{\phi}}_{\rm des} = -12\,{\rm deg/year}$, the simulations show that the electrochromic system must be switched on 160 days after the SD deployment (that is, $t_{\rm on} \simeq 0.44\,T_c$, see Fig. 4(a)) and maintained operating for about 143 days, until $t_{\rm off} \simeq 0.83\,T_c$. In this case the time interval necessary to complete the phasing maneuver is $\Delta t \simeq 1.27\,T_c$, the time variation of the state variables is drawn in Fig. 5(a), while the corresponding trajectory is shown in Fig. 5(b).

Conclusions

The current technological level is compatible with the miniaturization of the electro-mechanical components and the realization of a fascinating spacecraft concept called Smart Dust. The electrochromic material coated on its external surfaces allows the Smart Dust trajectory to be actively controlled, thus opening new mission options such as the in-orbit repositioning along a circular orbit. The intrinsic limit of this technology is, of course, in the extremely reduced payload mass that can be stowed on board. Nevertheless, the possibility of loading a number of Smart Dusts within a single conventional spacecraft may offer an interesting option for dropping the launch costs, especially in case of deep-space missions. The results presented in this Note describe, in analytical form, the relative linearized dynamics between a Smart Dust and a Mother Ship under the assumption of small relative distance between the two spacecraft compared to their distance from the Sun. The obtained analytical relations allow the orbital phasing problem of the Smart Dust to be solved with a simplified control law when the control system performs a single working cycle. A natural extension of this work is to consider a more complex problem, in which the control law is described by several working cycles, and whose solution requires an optimal approach for calculating the mission performance.

References

[1] Barnhart, D. J., Vladimirova, T., and Sweeting, M. N., "Satellite-on-a-chip development for future distributed space missions," *Proceedings of MNT for Aerospace Applications, CANEUS2006*, 27 August – 1 September 2006.

[2] Barnhart, D. J., Vladimirova, T., and Sweeting, M. N., "Very-small-satellite design for distributed space missions," *Journal of Spacecraft and Rockets*, Vol. 44, No. 6, 2007, pp. 1294–1306. doi: 10.2514/1.28678.

[3] Colombo, C., Lücking, C., and McInnes, C. R., "Orbit evolution, maintenance and disposal of SpaceChip swarms through electro-chromic control," *Acta Astronautica*, Vol. 82, No. 1, 2013, pp. 25–37. doi: 10.1016/j.actaastro.2012.05.035.

[4] Lücking, C., Colombo, C., and McInnes, C. R., "Electrochromic orbit control for smart-dust devices," *Journal of Guidance, Control, and Dynamics*, Vol. 35, No. 5, 2012, pp. 1548–1558. doi: 10.2514/1.55488.

[5] Colombo, C. and McInnes, C. R., "Orbital dynamics of "Smart-Dust" devices with solar radiation pressure and drag," *Journal of Guidance, Control, and Dynamics*, Vol. 34, No. 6, 2011, pp. 1613–1631. doi: 10.2514/1.52140.

[6] Colombo, C., Lücking, C., and McInnes, C. R., "Orbital dynamics of high area-to-mass ratio spacecraft with J_2 and solar radiation pressure for novel Earth observation and communication services," *Acta Astronautica*, Vol. 81, 2012, pp. 137—50. doi: 10.1016/j.actaastro.2012.07.009.

[7] Colombo, C. and McInnes, C. R., "Orbit design for future SpaceChip swarm missions in a planetary atmosphere," *Acta Astronautica*, Vol. 75, 2012, pp. 25–41. doi: 10.1016/j.actaastro.2012.01.004.

[8] Atchison, J. A. and Peck, M. A., "A passive, sun-pointing, millimeter-scale solar sail," *Acta Astronautica*, Vol. 67, No. 1-2, July-August 2010, pp. 108–121. doi: 10.1016/j.actaastro.2009.12.008.

[9] McInnes, C. R., "A continuum model for the orbit evolution of self-propelled 'smart dust' swarms," *Celestial Mechanics and Dynamical Astronomy*, Vol. 126, No. 4, November 2016, pp. 501–517. doi: 10.1007/s10569-016-9707-y.

[10] Manchester, Z., Peck, M., and Filo, A., "KickSat: A Crowd-Funded Mission to Demonstrate the World's Smallest Spacecraft," *AIAA/USU Conference on Small Satellites*, Logan, Utah, August 2013, Paper SSC13-IX-5.

[11] Jones, N., "First flight for tiny satellites," *Nature*, Vol. 534, No. 7605, June 2016, pp. 1516. doi: 10.1038/534015a.

[12] Mengali, G. and Quarta, A. A., "Heliocentric Trajectory Analysis of Sun-pointing Smart Dust with Electrochromic Control," *Advances in Space Research*, Vol. 57, No. 4, February 2016, pp. 991–1001. doi: 10.1016/j.asr.2015.12.017.

[13] McInnes, C. R., "Azimuthal Repositioning of Payloads in Heliocentric Orbit Using Solar Sails," *Journal of Guidance, Control, and Dynamics*, Vol. 26, No. 4, July–August 2003, pp. 662–664. doi: 10.2514/2.5098.

[14] Mengali, G. and Quarta, A. A., "In-orbit repositioning of multiple solar sail spacecraft," *Aerospace Science and Technology*, Vol. 12, No. 7, October 2008, pp. 506–514. doi: 10.1016/j.ast.2007.12.003.

[15] Quarta, A. A. and Mengali, G., "Optimal Solar Sail Phasing Trajectories for Circular Orbit," *Journal of Guidance, Control, and Dynamics*, Vol. 36, No. 6, November-December 2013, pp. 1821–1824. doi: 10.2514/1.59372.

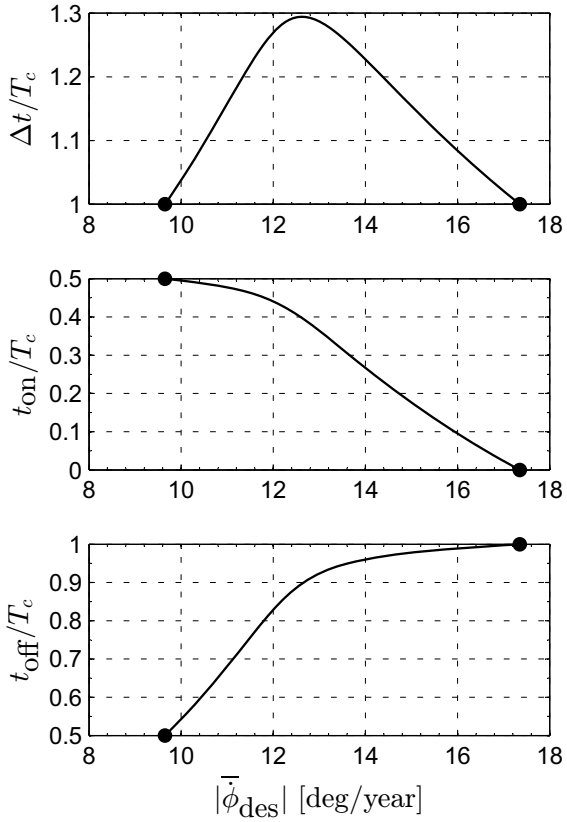

a) Phasing time and switching instants.

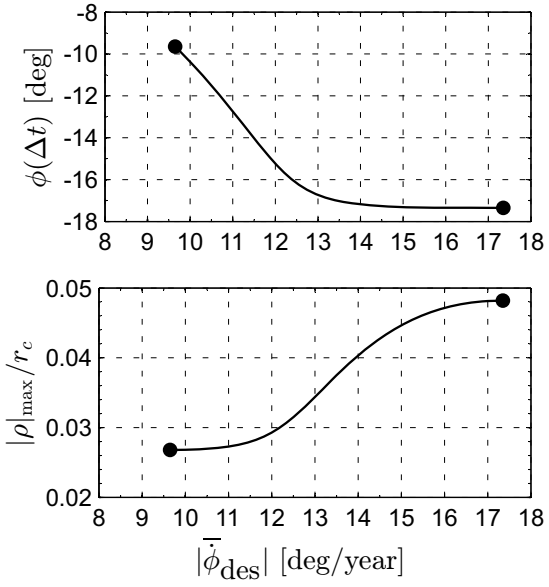

b) Phasing angle and maximum radial displacement.

Figure 4 Phasing performance as a function of $\overline{\dot{\phi}}_{\rm des}$ for the SD_1. Black circles refer to a constant lightness number.

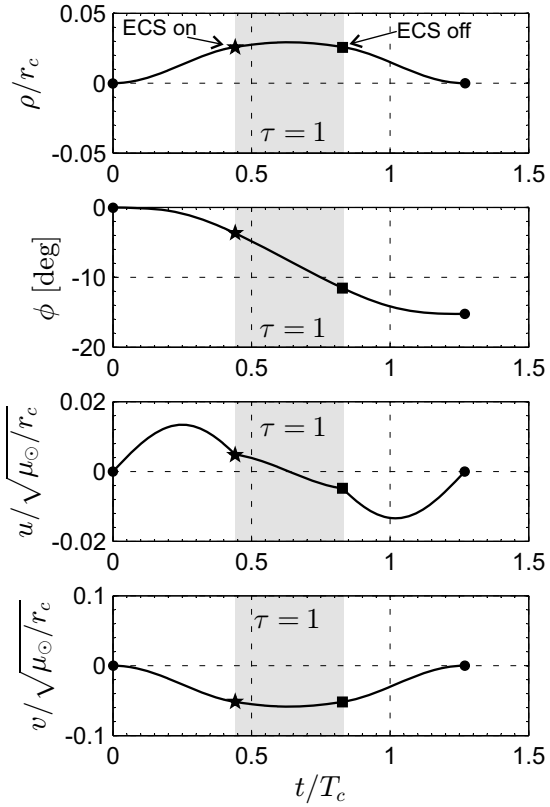

a) State variables.

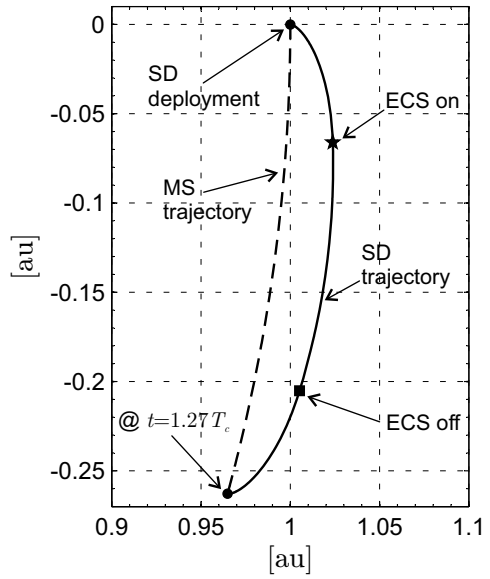

b) Relative trajectory.

Figure 5 Simulation results for the low-performance SD$_1$ case with $n = 1$ and $\bar{\dot{\phi}}_{\rm des} = -12\,\mathrm{deg/year}$.